BOLETIN DE LA SOCIEDAD ESPAÑOLA DE
Cerámica y Vidrio
www.elsevier.es/bsecv

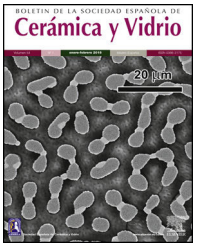

Performance of graphene oxide-modified electrodeposited ZnO/Cu_2O heterojunction solar cells

Nelly Maria Rosas-Laverde[a,b], *Alina Pruna*[a,c,*], *Jesus Cembrero*[a], *Javier Orozco-Messana*[a], *Francisco Javier Manjón*[d]

[a] *Department of Materials and Mechanical Engineering, Universitat Politècnica de València, Valencia, Spain*
[b] *Department of Materials, Escuela Politécnica Nacional, Quito, Ecuador*
[c] *Center for Surface Science and Nanotechnology, Polytechnic University of Bucharest, Bucharest, Romania*
[d] *Instituto de Diseño para la Fabricación y Producción Automatizada, Universitat Politècnica de València, 46022 Valencia, Spain*

ARTICLE INFO

Article history:
Received 19 December 2018
Accepted 17 June 2019
Available online 4 July 2019

Keywords:
Electrochemical deposition
ZnO
Cu_2O
Solar cells

ABSTRACT

We report the fabrication of ZnO/Cu_2O heterojunction solar cells by means of the electrodeposition technique. The effect of electrolyte medium for the ZnO deposition, annealing treatment and interface modification with graphene oxide (GO) layer on the photoelectrical properties was analyzed. The electrochemical results indicated a markedly dependent Cu_2O film electrodeposition on the GO-modified ZnO films. The modification of ZnO/Cu_2O interface with GO nanosheets and annealing treatment results in improved interface properties, varying morphology and defects in ZnO lattice that further lead to enhanced performance of the proposed heterojunction solar cells. While the obtained results indicate that the properties of GO coating need to be tailored for improved performance, a synergetic effect of the GO addition and annealing treatment on the photoelectric properties of the electrodeposited heterojunction is achieved.

Rendimiento de las celdas solares de heterounión ZnO/Cu_2O modificadas con óxido de grafeno

Palabras clave:
Deposición electroquímica
ZnO
Cu_2O
Celdas solares

RESUMEN

Se presenta la fabricación de celdas solares de heterounión de ZnO/Cu_2O obtenidas mediante la técnica de electrodeposición. Se analizó el efecto del electrolito utilizado para la deposición de ZnO, el tratamiento térmico aplicado y la modificación de la interfaz con una capa de óxido de grafeno (GO) sobre las propiedades fotoeléctricas. Los resultados electroquímicos indicaron que existe una marcada dependencia de electrodeposición de capa

* *Corresponding author.*
E-mail address: ai.pruna@gmail.com (A. Pruna).
https://doi.org/10.1016/j.bsecv.2019.06.002

de Cu_2O sobre las películas de ZnO modificadas con GO. La modificación de la interfaz ZnO/Cu_2O con nanohojas de GO y el tratamiento térmico dan como resultado mejoras en las propiedades de la interfaz, una morfología variable y defectos en la red de ZnO que conducen a un mejor rendimiento de las celdas solares de heterounión propuestas. Si bien los resultados obtenidos indican que las propiedades del recubrimiento de GO deben adaptarse para mejorar el rendimiento, se logra un efecto sinérgico del tratamiento de adición y térmico de GO aplicados sobre las propiedades fotoeléctricas de la heterounión electrodepositada.

Introduction

The need for using alternative energy sources to substitute fossil fuel worldwide has led to the investment in research and development of new materials and methods [1]. The photovoltaic solar cells (PVs) convert solar energy into electricity and represent the most important solar active technology [2]. In order to improve the efficiency of solar cells, various techniques considering different aspects have been employed. Given its high efficiency to convert solar energy into electricity [3], most PVs are based on silicon; however, they also imply a high cost [4]. Other technologies include organic, dye-sensitized and thin film PVs. Amongst these technologies, thin film ZnO/Cu_2O heterojunction PVs have lately attracted much interest [5] as a candidate for the next generation thin film PVs thanks to its non-toxicity, abundance, absorption coefficient higher than single crystalline Si and a theoretical conversion efficiency around 18% [6,7].

ZnO/Cu_2O heterojunction PVs can be fabricated by various methods such as, thermal oxidation, chemical vapor deposition, plasma evaporation, magnetron sputtering, pulsed laser deposition and electrochemical deposition (ECD) [8,9]. ECD involves the electrodeposition of ZnO layer onto a transparent conducting oxide (TCO) glass, followed by the electrodeposition of the Cu_2O layer resulting in a basic structure as TCO glass/ZnO_{ECD}/Cu_2O_{ECD}/contact electrode [5].

In PVs prepared by ECD, the ZnO layer can be used as the TCO window layer [2] since ZnO is an intrinsic n-type semiconductor with a wide band gap of 3.3 eV [2,10]. Films of ZnO can be prepared by chemical vapor deposition, atomic layer deposition, radio frequency magnetron sputtering and also by ECD techniques [11]. ECD is a preferred technique for thin film deposition as it allows the deposition of homogeneous films with specific crystal structure. On the other hand, cuprous oxide (Cu_2O) is a native p-type semiconductor characterized by a band gap of 2 eV [12] and can be employed as an absorber layer [3] thanks to its high absorption coefficient [5]. Cu_2O has been considered as material for photovoltaic applications also thanks to its non-toxicity, abundance [12,13], and low-cost manufacturing process [4]. Amongst the fabrication techniques sputtering deposition, thermal oxidation of a metallic Cu sheet and ECD have been widely employed [4,5,10].

So far, ZnO/Cu_2O heterojunction PVs have never reached high efficiencies in practice [7]. Actually, ZnO/Cu_2O heterojunction PVs have only reached a power conversion efficiency (*PCE*) of 1.43% fabricated by ECD [14]. This lower *PCE* is related with the quality of structures of ZnO and Cu_2O layers, and is mainly due to defects and existing high state density in the ZnO/Cu_2O interface that may produce recombination process [15–17].

In order to improve the performance of ZnO/Cu_2O heterojunction PVs, the interaction between ZnO and Cu_2O has a paramount importance. This interaction is governed by the properties of the films derived from the deposition methods. Jeong et al. showed an important effect of the ECD conditions (pH and temperature) on the performance of ZnO/Cu_2O heterojunction PVs. On the other hand, Atwater et al. showed that interface stoichiometry is a "must" for such PVs [18,19]. Finally, Fujimoto et al. demonstrated that the performance of ZnO/Cu_2O heterojunction PVs is highly related to the type of hydroxide (LiOH, KOH, and NaOH) employed at the preparation of electrolyte for the Cu_2O deposition [14]. They found that the *PCE* improved by using LiOH with respect to NaOH and KOH, reaching the values of 1.43, 0.698 and 0.591%, respectively. These results are attributed to the presence of ~100 nm Cu_2O nanocrystals with the highest specific orientation plane (111) when using LiOH. Other works showed different crystal orientation for Cu_2O, such as (200), (110), and (111) by varying the bath pH from 8.69, 9.10, to 10.34, respectively. In this context, the orientation plane (111) was found the best Cu_2O crystal orientation for improving the *PCE* in ZnO/Cu_2O heterojunction PVs since its produces less defects and improves light collection efficiency [20]. Other approach applied for improving the performance of those PVs considered the addition of a graphene layer at the ZnO/Cu_2O interface, so as to act as an electron mediator in order to reduce the recombination of photogenerated charges [15] or the use of graphene oxide in a reduced form by thermal process [21].

Given the unique properties of graphene including near transparency, almost no band gap and light absorption across a broad spectrum, graphene has attracted great attention for its use in PVs [22]. Graphene's oxidized form, graphene oxide (GO) represents a cheaper alternative to graphene which is more easy to handle in solution-process, as it is decorated with oxygen functional groups which confer it with hydrophilicity and great potential for composite applications [23]. Li et al. showed that the incorporation of GO could suppress leakage current and reduce recombination via efficient hole transporting and electron blocking; thus resulting in improvement of power conversion efficiency of planar heterojunction PVs [24]. However, while the oxygen groups confer GO with hydrophilicity, they result in low conductivity which indicates that at least a partial removal of the oxygen groups is advised in order to achieve better conductivity. The reduced graphene oxide

(rGO) can be obtained by chemical, thermal or hydrothermal reduction technique.

In this work, we report on the influence of GO incorporation and annealing treatment on the properties of the ZnO/Cu_2O interface obtained by the ECD technique in order to improve the performance of the corresponding heterojunction solar cell. To the best of our knowledge, this study represents the first one on the combined effect of GO incorporation and the electrochemical growth conditions, such as aqueous and organic media and ZnO precursor. The obtained results suggest that such approach shows a great potential in improving the performance of ZnO/Cu_2O heterojunction PVs.

Materials and methods

Materials

Zinc chloride ($ZnCl_2$), potassium chloride (KCl), copper (II) sulphate pentahydrate ($CuSO_4{\cdot}5H_2O$, 85%), lactic acid ($C_3H_6O_3$, 85%), sodium hydroxide (NaOH) and dry dimethyl sulfoxide (DMSO) were purchased from Alfa Aesar. All chemicals were reagent grade and used as received. Graphene oxide (GO) was purchased from Sigma Aldrich. Fluorine-doped tin oxide (FTO) coated glass (15 Ω/sq.) was employed as substrate. Prior to the depositions, the FTO substrates were cleaned successively in detergent solution, deionized water and isopropanol in ultrasonic bath for 15 min each. Finally, the substrates were rinsed with ethanol and dried under N_2 atmosphere.

Fabrication of ZnO/Cu_2O heterojunction

ZnO and Cu_2O films were deposited by a conventional three-electrode ECD method using a potentiostat (PGSTAT 101 AUTOLAB) and NOVA software. A conventional three electrode glass cell using a working electrode (FTO substrate), a counter-electrode (Pt foil) and a reference electrode (Ag/AgCl in saturated KCl) were used.

Deposition of ZnO films

A factorial experimental design generating 8 samples was considered in order to minimize the duration of experiments. The conditions of the deposition are summarized in Table 1. Three parameters were investigated: the medium (parameter A), an annealing treatment (parameter B) and absence/presence of GO (parameter C), generating 8 samples denominated with the levels of each parameter (ABC). The effect of aqueous and organic media in the solution on the performance of the heterojunction was studied by using either H_2O or DMSO as solvent [25–28]. ZnO films were deposited onto the FTO substrate by the ECD method using a solution comprising zinc precursor 5×10^{-3} M $ZnCl_2$, supporting electrolyte 0.1 M KCl and saturated with O_2 as oxygen precursor. In the case of organic medium, a saline bridge was employed for contacting the electrolytic cell with the reference electrode. The electrolyte was maintained at 75 °C using a thermostatic bath. The pH value of the prepared solution was 6. The electrochemical deposition was performed at a constant potential of −0.8 V for 30 min [29].

Table 1 – Control variables and corresponding work levels.

Variable	Code	Lower level (−)	High level (+)
Medium	A	H_2O	DMSO
Heat treatment (HT)	B	Without	With
GO	C	Without	With

In order to modify the ZnO/Cu_2O interface, the ZnO films were coated with GO films by dip-coating method. In this respect, the GO solution (0.1 mg/ml) was sonicated for 10 min. The GO coating was achieved by immersing the substrate in the GO solution for 3 min, rinsing with distilled water and drying with air.

For improving the crystallinity of ZnO layer and observe the effect of reduction in GO coating on the performance of the heterojunction, a thermal treatment (HT) at 350 °C for 60 min was applied before depositing the Cu_2O layer. Thus, the non-annealed ZnO-based heterojunction (B at low level) with/without GO shows the effect of GO and the annealing of ZnO modified with GO shows the effect of reduced GO (rGO).

Deposition of Cu_2O films

Cu_2O films were prepared by the ECD method using a solution consisting of 0.4 M $CuSO_4$, 3 M $C_3H_6O_3$, and 4 M NaOH. The ZnO/FTO substrates with and without GO were employed as the working electrode. The electrodeposition was performed at 35 °C at a constant potential of −0.6 V for 120 min [30]. Finally, the substrates were rinsed with water and dried with air.

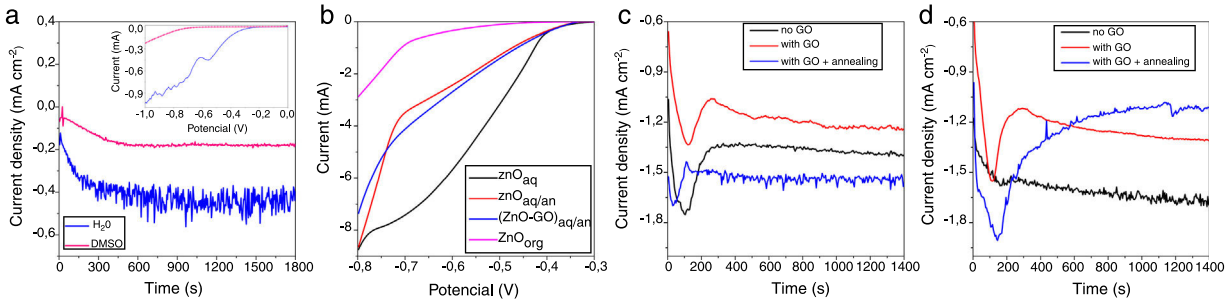

Fig. 1 – Chronoamperometric curves for deposition of ZnO films (linear scan voltammograms in inset) – (a); linear scan voltammograms for Cu_2O deposition onto ZnO films – (b); Chronoamperometric curves for deposition of Cu_2O films in aqueous (c) and organic media (d).

Characterization

The structural properties of the films were characterized by X-ray diffraction (XRD) using a Rigaku Ultima IV diffractometer in the Bragg-Bentano configuration using Cu Kα radiation (1.54 Å). The diffraction peaks from the ZnO and Cu_2O were indexed with reference to the JCPDS diffraction files. The morphology was analyzed by using Field Emission Scanning Electron Microscopy (FESEM) Bruker working at a 2 kV. Focused Ion Beam (FIB, Bruker) milling was employed to analyze the cross-section of the heterojunction. The vibrational properties of the films were characterized by Raman spectroscopy using a HORIBA Jobin Yvon LabRam HR UV microspectrometer using a He–Ne (632.8 nm) laser with a 1.6 cm^{-1} resolution. Finally, the photoelectrical properties were studied with a potentiostat (PGSTAT 302N AUTOLAB) equipped with AM 1.5G illumination from a calibrated solar simulator with irradiation intensity of 100 mW cm^{-2}. The top coating of conductive carbon cement (Leit-C) was deposited on the heterojunctions.

Results and discussion

In order to investigate the formation ZnO film, linear scan voltammetry was applied for both media (see inset in Fig. 1a). It can be observed that the nucleation of ZnO is slightly slower in the organic medium however, the deposition can be performed in both cases at a potential value of −0.8 V. Further, the ECD current transients for deposition of ZnO were recorded [31,32] as depicted in Fig. 1a and, while the chronoamperometric curves in Fig. 1a show similar behaviour irrespectively of the solvent, the deposition plateau current in organic medium appears lower than in aqueous medium, in agreement with the linear scans. The first stage of the ECD curves corresponds to the formation of nuclei, followed by the growth stage where the current density reaches a plateau value [33]. The nucleation process occurs during the first 200 and 400 s in the aqueous and organic solvent, respectively. The aqueous solvent enhances the formation of nuclei as it can be seen from the corresponding slope. On the other hand, the more stable trend of the EDC curve indicates that the organic medium results in a more homogeneous growth of the nuclei, while in aqueous medium the unstable evolution indicates varying growth of the formed nanostructures. The current plateau stabilizes at an increased value in the aqueous medium with respect to the organic one (0.42 mA cm^{-2} vs. 0.17 mA cm^{-2}) which is indicative of a thicker film formation.

Further, the linear scan voltammograms for the deposition of Cu_2O films onto the ZnO layers previously obtained in varying conditions were recorded as depicted in Fig. 1b. While the nucleation varies according to the surface properties induced in the ZnO layer according to each condition (medium, annealing, presence of rGO), a potential value of −0.6 V can be applied for the deposition of Cu_2O films in all cases. The electrode reaction which governs the electrodeposition of Cu_2O is [10,34,35]:

$$2Cu^{2+} + 2e^- \rightarrow 2Cu^+$$

$$2Cu^+ + 2OH^- \rightarrow 2Cu(OH)$$

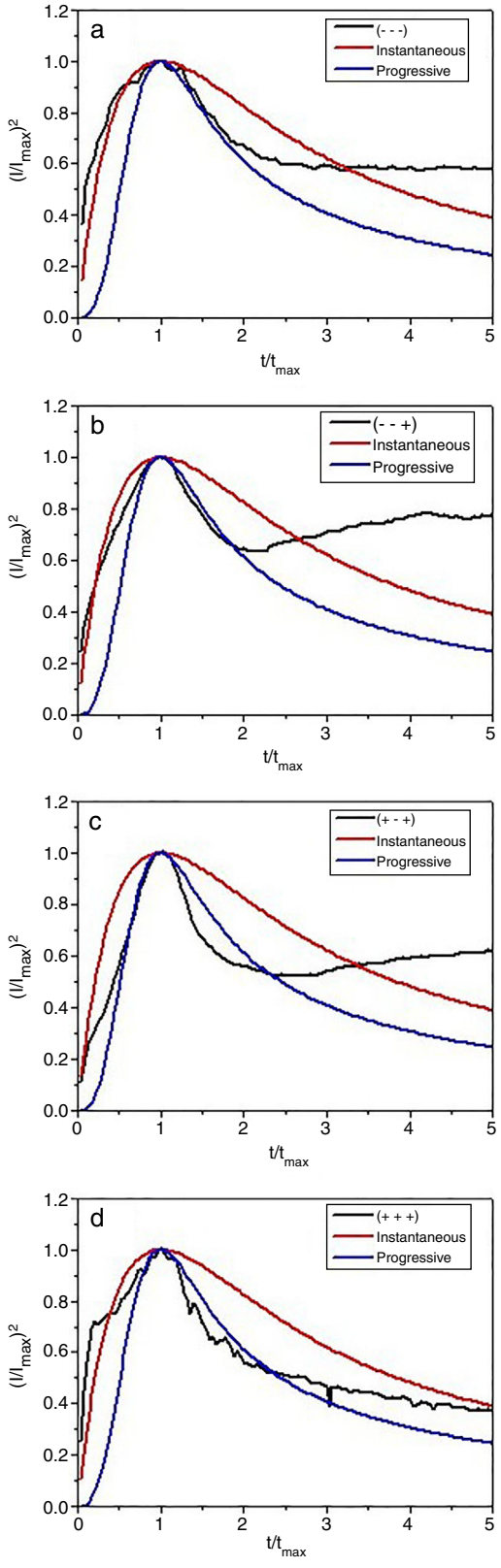

Fig. 2 – Non dimensional plots $(I/I_{max})^2$ vs. (t/t_{max}) for the electrodeposition of Cu_2O films from aqueous media onto ZnO (a) and GO-modified ZnO substrate (b) and from organic media onto GO-modified ZnO without (c) and after annealing (d).

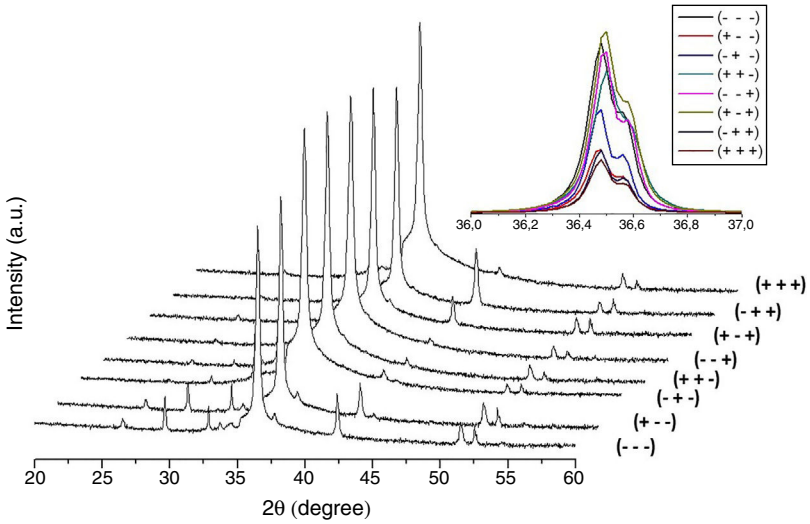

Fig. 3 – XRD spectra of a Cu_2O/ZnO heterojunction onto FTO substrates.

$$2Cu(OH) \rightarrow Cu_2O + H_2O$$

Fig. 1c and d depicts the corresponding chronoamperometric curves for the ECD of Cu_2O films at the surface of the ZnO substrate obtained in aqueous and organic solvents, as a function of GO and annealing treatment. As shown in Fig. 1c and d, the nucleation zone for the ECD of Cu_2O films occurs before 200 s either using an aqueous or organic solution. In the absence of the GO coating, the ECD of Cu_2O at the surface of ZnO layer results in a current density plateau of $-1.4\,mA\,cm^{-2}$ ($-1.7\,mA\,cm^{-2}$) when the ZnO layer is deposited using aqueous (organic) solvent. This can be attributed to a lower lattice mismatch between Cu_2O and the ZnO obtained in organic medium, which further results in improved Cu_2O growth. On the other hand, the GO coating at the surface of ZnO films induces a lower Cu_2O growth current density (thinner Cu_2O film) than in its absence due to its insulating properties, e.g. about $-1.23\,mA\,cm^{-2}$ for both ZnO layers grown using aqueous and organic solvents. Nevertheless, the decrease in current is indicative of the efficient coating with GO film. The annealing treatment of the GO-modified ZnO layer induced an enhanced growth of Cu_2O film in both solvents. Thus, in aqueous medium the annealing of the GO-modified ZnO substrate resulted in lower nucleation duration for Cu_2O below 100 s and an increased growth current plateau ($-1.5\,mA\,cm^{-2}$). This can be attributed to improved crystalline structure of ZnO upon annealing treatment [10] and conductivity properties of reduced GO due to partial removal of oxygen functional groups by thermal reduction, as well as to the residual oxygen functional groups in GO employed as nucleation sites. In the case of the ZnO layer obtained with organic solvent, the annealing results in longer nucleation duration and decreased current plateau. This could be attributed to the smaller roughness of the ZnO layer obtained from organic medium, which offers less nucleation sites for Cu_2O formation.

The above-mentioned results are confirmed by the non dimensional plots $(I/I_{max})^2$ vs. (t/t_{max}) of the chronoamperometric curves (see Fig. 2). In order to obtain more information on the nucleation and growth of Cu_2O as a function of ZnO properties and GO addition, the current transients were compared to the Scharifker and Hills tridimensional theoretical model [36]. As it can be observed, at $t/t_{max} < 1$, the experimental curve follows the instantaneous 3D model during the electro-crystallization process followed by a progressive one for the bare aqueous-based ZnO film. On the other hand, the GO addition turns the process into a progressive one, which is attributed to the use of oxygen functional groups in GO as nucleation sites. The same effect of GO is also observed in the case of the organic-based ZnO film with and without the thermal annealing treatment.

The crystalline structure of the electrodeposited ZnO and Cu_2O layers was studied by XRD measurements. Fig. 3 shows the XRD spectra of the Cu_2O/ZnO heterojunction electrodeposited in different conditions. The obtained spectra appear to be similar for all the samples independently of the experimental conditions. The reflections in the XRD pattern confirmed the deposition of polycrystalline ZnO thin films with hexagonal crystal structure and (101) preferential orientation. Other peaks such as (100) were identified as well (JCPDS 00-036-1451) [37]. On the other hand, the Cu_2O layers showed a strong intensity of the (111) peak, which indicates a preferential orientation in agreement with other studies on potentiostatic electrochemical deposition of Cu_2O [10]. Other reflections were (110), (200) and (211) in agreement with the PDF file JCPDS 00-005-0667 [38]. The growth of Cu_2O with (111) preferential orientation on the top of ZnO films with the (101) orientation indicates a good crystallographic matching [3]. The interfacing between Cu_2O and ZnO layers is indicated by the overlapping of a ZnO (101) diffraction peak with a Cu_2O (111) diffraction peak, as seen in inset in Fig. 3. In absence of GO, the annealing treatment results in more intense reflection peaks of the heterojunction component layers. Upon GO addition, the annealing results in lower intensity of the peaks, which is in agreement with the electrodeposition results indicating the deposition of thinner films in the presence of GO. No other diffraction peaks, except those of the FTO substrate at 26.49°, 51.52° [4], could be observed, indicating the adequacy of the

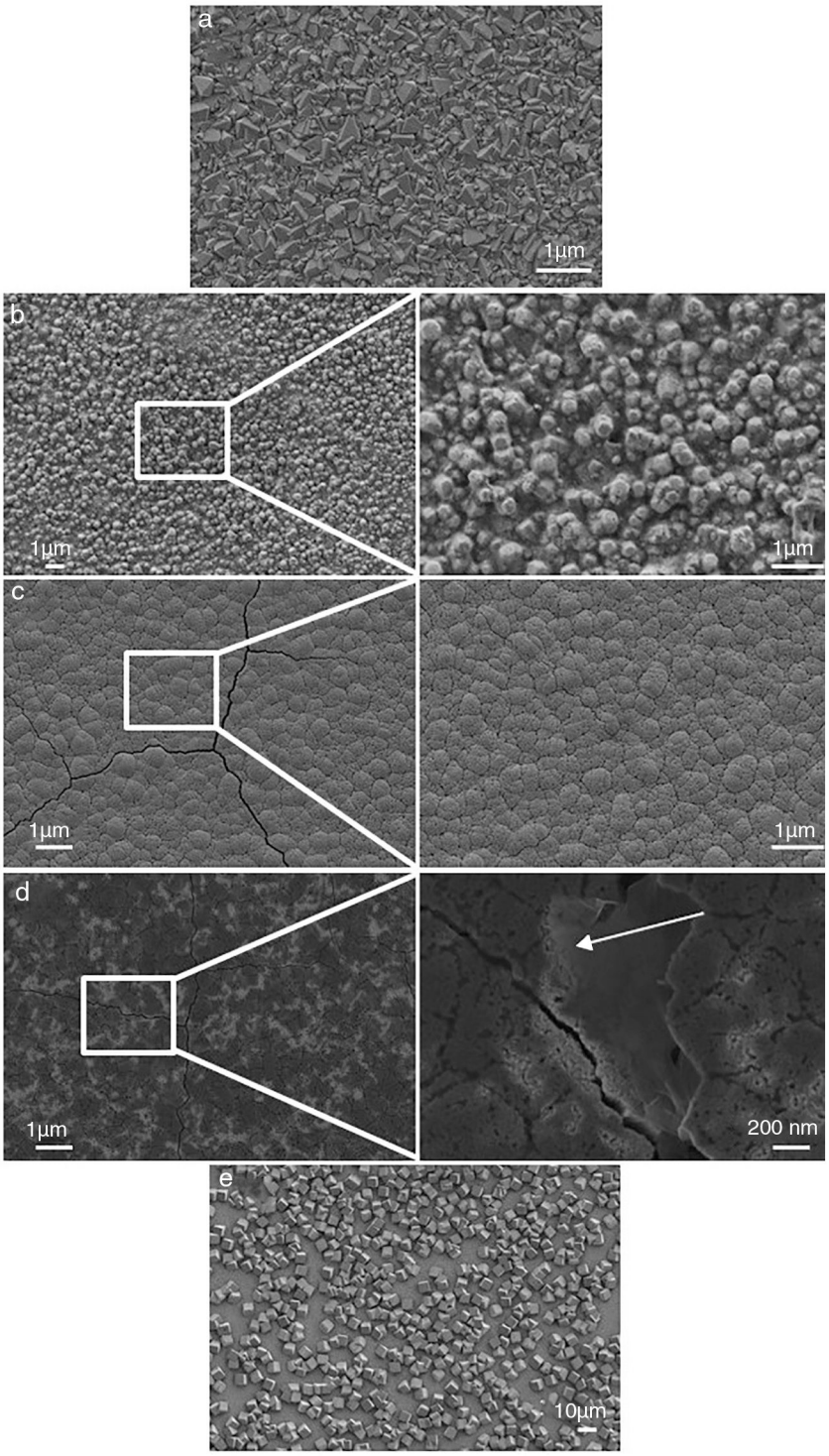

Fig. 4 – Typical morphology of FTO substrate (a), ZnO electrodeposited from aqueous electrolyte (b and inset), ZnO electrodeposited from organic electrolyte (c and inset), rGO-modified ZnO layer (d and inset) and typical morphology of Cu_2O (e).

deposition parameters for the fabrication of the given heterojunction.

The morphology of the obtained films was analyzed by means of FESEM microscopy. Fig. 4a shows the typical morphology of FTO substrate employed for the fabrication of the heterojunctions, where the textured FTO film presents homogeneously dispersed large grains and high roughness, as reported elsewhere [39]. Besides the FTO surface roughness, the type of electrodeposition medium greatly affects the morphology of the ZnO layers deposited at the surface of FTO substrate, as depicted in Fig. 4b and c showing representative ZnO morphologies obtained from aqueous and organic media,

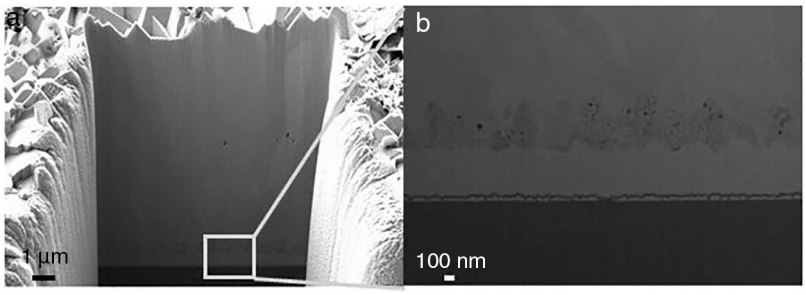

Fig. 5 – Cross-section of the ZnO/Cu_2O heterojunction (a) and higher magnification showing the ZnO layer and ZnO/Cu_2O interface (b).

Table 2 – Thickness of ZnO and Cu_2O layers (FIB measurements).

Sample (ABC)	ZnO thickness (nm)	Cu_2O thickness (μm)
− + −	536	9.9
+ + −	521	10.5
− + +	543	8.9
+ + +	552	9

respectively. There is an obvious shift of the nanostructured rod-like morphology with large diameter from the aqueous electrolyte to the thinner coalesced rods from the organic one [40]. The presence of GO nanosheets is further evidenced from the exemplificative images in Fig. 4d and inset (arrow), depicting the GO-modified ZnO film upon annealing treatment at the surface of ZnO layer. The non-continuous GO coating can be explained by the different behaviour of the internal structure of ZnO and GO with the applied temperature and by the partial removal of oxygen groups in GO causing increasing hydrophobicity of the nanosheets. Lastly, the typical cube-like morphology of the Cu_2O layer is presented in Fig. 4e [30].

Fig. 5 further depicts a typical cross-section of the ZnO/Cu_2O heterojunctions and the thickness values of each layer as a function of synthesis conditions are presented in Table 2. It can be observed that ZnO film thickness is only slightly affected by the deposition medium. The presence of rGO material at the interface reduces the Cu_2O thickness with about 1 μm, which is attributed to the residual oxygen groups in rGO inducing lower conductivity. A strong interface effect can be clearly observed between the ZnO and Cu_2O layer.

Raman spectroscopy was employed to study the defects in ZnO host lattice grown in the different solutions as well as the influence of GO coating and upon annealing treatment. The Raman patterns of the singular components could be retrieved in the spectra of the GO-modified ZnO layer, confirming successful electrodeposition of ZnO film in both electrolytes and the modification of ZnO layer with GO nanosheets. The Raman spectra of ZnO grown from aqueous and organic electrolytes are shown in Fig. 6a and b, respectively. The typical Raman mode for hexagonal wurtzite-phase ZnO is observed at 437.9 cm^{-1}, in the layer obtained with aqueous electrolyte, coated by GO, and after annealing, and corresponds to non-polar optical phonon E_{2H} [41–43]. It must be noted that upon annealing and modification with GO coating, this peak is more clearly seen and also another peak close to 411 cm^{-1} is observed which could be related to the E_1(TO) mode of ZnO [42], thus indicating an increase of the crystalline quality with annealing. The peak shifts towards higher wavenumbers (445 cm^{-1}) and decreases in intensity which is indicative of disorder in the ZnO lattice [44]. The broad band centred at 538 cm^{-1} could be attributed to the TO + TA mode of hexagonal ZnO, but it is more likely related to the one-phonon density of states observed due to defect-assisted Raman scattering [43]. It is also frequently related to the defects including oxygen vacancies and interstitial zinc defect states [41] and it was observed to shift to 550 and 553 cm^{-1} along with an increase in intensity upon the annealing treatment and GO modification

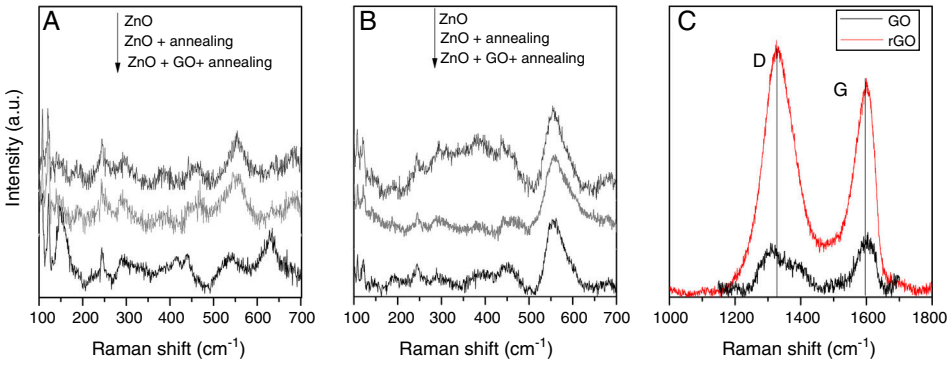

Fig. 6 – Raman spectra of ZnO layer electrodeposited from aqueous electrolyte (a) and from organic one (b) with and without annealing and modification with GO. (c) Raman spectra of GO coating before and after annealing.

Table 3 – Photoelectrical properties of heterojunction solar cells.

Sample (ABC)	V_{oc} (mV)	I_{sc} (μA)
– – –	56.7	130.9
+ – –	80.8	188.3
– + –	68.0	155.4
+ + –	57.7	298.0
– – +	49.7	125.6
+ – +	106.7	94.7
– + +	66.7	158.3
+ + +	121.4	92.0

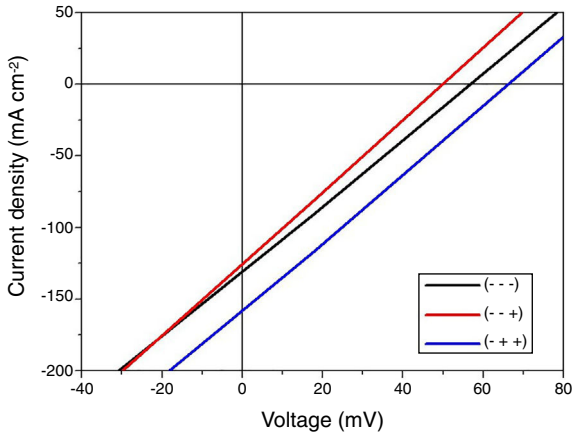

Fig. 7 – Typical *I–V* curves for the ZnO/Cu_2O heterojunction cells.

of the ZnO obtained from aqueous electrolyte. These results are in strong agreement with other studies reporting increased defects in ZnO upon hybridization with GO [45,46]. The broad band at 631 cm^{-1}, attributed to TA + LO or more specifically to TA + B_{1H} in [43,47], appears in ZnO after annealing treatment and coating with GO. As can be seen in Fig. 6b, the use of organic electrolyte resulted in similar Raman features for ZnO layers, but a clearly more intense peak was observed at 553 cm^{-1} pointing towards an increased level of defects in the ZnO lattice. This means that ZnO quality is worse when using organic than aqueous solution.

The evolution of structural information in the GO nanomaterials with the annealing treatment was retrieved from the Raman spectrum presented in Fig. 6c. The typical bands in the GO are present; i.e. the G mode at 1598 cm^{-1}, corresponding to the sp^2 hybridized carbon, and the D mode at 1320 cm^{-1}, which is activated by the defects in the carbon network and can be observed in the spectra of all modified layers [41]. Upon annealing, the GO nanosheets are thermally reduced to rGO by partial removal of oxygen groups and exhibit a lower intensity ratio between the D and G bands which indicates a healing process for the graphitic domains.

The effect of interface properties induced by electrodeposition medium, annealing treatment and modification with GO on the photoelectrical features of the heterojunction PVs was analyzed and the results are presented in Table 3. Typical *I–V* curves are depicted in Fig. 7. As it can be observed, the annealing treatment resulted in increased V_{oc} for the cells with ZnO obtained from aqueous medium and were attributed to the improvement in ZnO conductivity due to a higher crystalline quality. Although in presence of GO the open-circuit voltage (V_{oc}) slightly decreased, upon annealing it resulted in a larger increment of V_{oc} value. This effect can be attributed to the improved conductivity properties of rGO with respect to GO, as some of the oxygen groups were removed by thermal treatment. The annealing treatment resulted in similar effect on the short-circuit current (I_{sc}) trend. The results indicated the use of both GO and annealing treatment resulted in the highest photoelectric parameters, which are attributed to the reduced recombination at the interface.

On the other hand, the use of organic medium for the electrodeposition of ZnO layer resulted in higher V_{oc} values for the corresponding conditions than the use of aqueous medium. This result can be explained by the difference in morphology and increased defects in ZnO layer grown with organic medium, which further affects the ZnO/Cu_2O interface properties.

Finally, the effect of a different ZnO precursor, namely, $Zn(NO_3)_2$, in the ECD process was studied. $Zn(NO_3)_2$ serves as a precursor for both Zn^{2+} and OH^- ions required for the formation of ZnO. XRD measurements (Fig. 8a) showed that the structural properties of the ZnO layer electrodeposited from nitrate precursor are similar to those from $ZnCl_2$ since the XRD pattern exhibits similar characteristics. On the other hand, Raman spectroscopy measurements of the ZnO electrodeposited from nitrate precursor and further modified with GO coating (Fig. 8b) show similar features as the ones in Fig. 7. However, the FESEM images in Fig. 9 revealed a plate-like morphology for the ZnO film electrodeposited

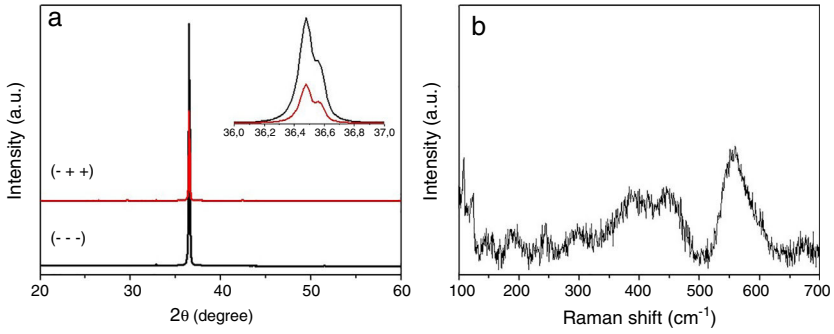

Fig. 8 – Typical XRD spectra of ZnO/Cu_2O heterojunction (a) and Raman spectra of ZnO layer obtained from $Zn(NO_3)_2$ precursor and modified with GO coating (b).

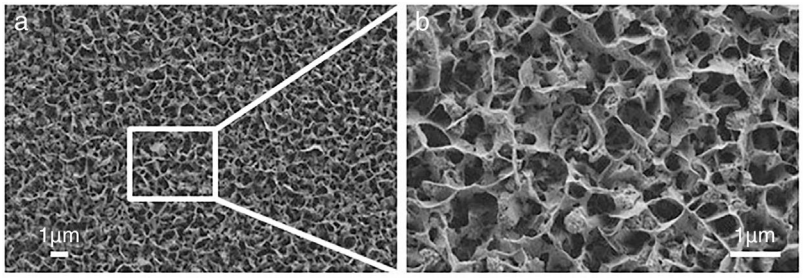

Fig. 9 – FESEM images of ZnO layer electrodeposited from $Zn(NO_3)_2$ precursor in aqueous media.

from the nitrate precursor. The photoelectric measurement indicated improved properties with respect to the PVs based on $ZnCl_2$-based non-annealed ZnO and in absence of GO. The heterojunction cell based on annealed GO-modified ZnO layer exhibited slightly lower V_{oc} value of 65.4 mV with respect to $ZnCl_2$-based counterpart, but an increased J_{sc} value of 220.5 μA cm^{-2}. The obtained results could be attributed to the interface properties due to the ZnO morphology.

Although the effect of GO addition and electrodeposition technique on the photoelectrical properties of the ZnO/Cu_2O heterojunction PV is complex, the approach followed in this work shows a synergetic effect of GO-modified interface and annealing treatment. However, the properties of GO coatings such as the thickness, continuity and reduction degree need to be optimized.

Conclusions

A study of ZnO/Cu_2O heterojunction PVs grown by ECD is reported. The effect of electrolyte medium, annealing treatment and interface modification with GO layer on the photoelectrical properties was analyzed. The electrochemical results indicated that thinner Cu_2O films grow on GO-modified ZnO films while annealing of GO-modified ZnO improves the subsequent electrodeposition of Cu_2O films. The modification of ZnO/Cu_2O interface with GO nanosheets and application of annealing treatment results in slightly increased photoelectrical properties for the heterojunction solar cells, due to the strong interface properties and the defects in ZnO lattice which reduce the recombination at interface. While the results indicate a synergy between the GO addition and annealing treatment for the electrodeposited heterojunction, the properties of GO coating need to be tailored for enhanced performance.

Acknowledgements

Financial support from Escuela Politécnica Nacional (project number PIMI 15-09), Secretaría de Educación Superior, Ciencia, Tecnología e Innovación (SENESCYT) of Ecuador, Romanian National Authority for Scientific Research and Innovation CNCS – UEFISCDI (project number PN-III-P1-1.1-TE-2016-1544), Spanish government MINECO (projects MAT2016-75586-C4-2-P and MAT2015-71070-REDC) and from Generalitat Valenciana (project PROMETEO 2018/123 – EFIMAT) is gratefully acknowledged. In addition, authors would like to thank to the Microscopy Service of UPV and Dr. David Busquets-Mataix for useful advice.

REFERENCES

[1] A. Kathalingam, D. Vikraman, H.S. Kim, H.J. Park, Facile fabrication of n-ZnO nanorods/p-Cu_2O heterojunction and its photodiode property, Opt. Mater. (Amst.) 66 (2017) 122–130, http://dx.doi.org/10.1016/j.optmat.2017.01.051.

[2] S. Panigrahi, D. Nunes, T. Calmeiro, K. Kardarian, R. Martins, E. Fortunato, Oxide-based solar cell: impact of layer thicknesses on the device performance, ACS Comb. Sci. 19 (2017) 113–120, http://dx.doi.org/10.1021/acscombsci.6b00154.

[3] H. Makhlouf, M. Weber, O. Messaoudi, S. Tingry, M. Moret, O. Briot, R. Chtoutou, M. Bechelany, Study of Cu_2O/ZnO nanowires heterojunction designed by combining electrodeposition and atomic layer deposition, Appl. Surf. Sci. 426 (2017) 301–306, http://dx.doi.org/10.1016/j.apsusc.2017.07.130.

[4] K. Cheng, Q. Li, J. Meng, X. Han, Y. Wu, S. Wang, L. Qian, Z. Du, Interface engineering for efficient charge collection in Cu_2O/ZnO heterojunction solar cells with ordered ZnO cavity-like nanopatterns, Sol. Energy Mater. Sol. Cells 116 (2013) 120–125, http://dx.doi.org/10.1016/j.solmat.2013.04.021.

[5] D.C. Perng, M.H. Hong, K.H.H. Chen, K.H.H. Chen, Enhancement of short-circuit current density in Cu_2O/ZnO heterojunction solar cells, J. Alloys Compd. 695 (2017) 549–554, http://dx.doi.org/10.1016/j.jallcom.2016.11.119.

[6] M. Zamzuri, J. Sasano, F.B. Mohamad, M. Izaki, Substrate type ⟨111⟩-Cu_2O/⟨0001⟩-ZnO photovoltaic device prepared by photo-assisted electrodeposition, Thin Solid Films 595 (2015) 136–141, http://dx.doi.org/10.1016/j.tsf.2015.10.054.

[7] X. Zhou, Y. Xie, J. Ma, H. Mi, J. Yang, J. Cheng, T.K.A. Hoang, Synthesis of hierarchical structure cuprous oxide by a novel two-step hydrothermal method and the effect of its addition on the photovoltaic properties of ZnO-based dye-sensitized solar cells, J. Alloys Compd. 721 (2017) 8–17, http://dx.doi.org/10.1016/j.jallcom.2017.05.334.

[8] O. Messaoudi, H. Makhlouf, A. Souissi, I. Ben assaker, G. Amiri, A. Bardaoui, M. Oueslati, M. Bechelany, R. Chtourou, Synthesis and characterization of ZnO/Cu_2O core–shell nanowires grown by two-step electrodeposition method, Appl. Surf. Sci. 343 (2015) 148–152, http://dx.doi.org/10.1016/j.apsusc.2015.03.045.

[9] X. Jiang, Q. Lin, M. Zhang, G. He, Z. Sun, Microstructure, optical properties, and catalytic performance of Cu_2O-modified ZnO nanorods prepared by electrodeposition, Nanoscale Res. Lett. 10 (2015) 2–7, http://dx.doi.org/10.1186/s11671-015-0755-0.

[10] S. Hussain, C. Cao, G. Nabi, W.S. Khan, Z. Usman, T. Mahmood, Effect of electrodeposition and annealing of ZnO on optical and photovoltaic properties of the p-Cu_2O/n-ZnO solar cells, Electrochim. Acta 56 (2011) 8342–8346, http://dx.doi.org/10.1016/j.electacta.2011.07.017.
[11] D. Kang, D. Lee, K.-S. Choi, Electrochemical synthesis of highly oriented, transparent, and pinhole-free ZnO and Al-doped ZnO films and their use in heterojunction solar cells, Langmuir 32 (2016) 10459–10466, http://dx.doi.org/10.1021/acs.langmuir.6b01902.
[12] J. Kaur, O. Bethge, R.A. Wibowo, N. Bansal, M. Bauch, R. Hamid, E. Bertagnolli, T. Dimopoulos, All-oxide solar cells based on electrodeposited Cu_2O absorber and atomic layer deposited ZnMgO on precious-metal-free electrode, Sol. Energy Mater. Sol. Cells 161 (2017) 449–459, http://dx.doi.org/10.1016/j.solmat.2016.12.017.
[13] W. Niu, M. Zhou, Z. Ye, L. Zhu, Photoresponse enhancement of Cu_2O solar cell with sulfur-doped ZnO buffer layer to mediate the interfacial band alignment, Sol. Energy Mater. Sol. Cells 144 (2016) 717–723, http://dx.doi.org/10.1016/j.solmat.2015.10.013.
[14] K. Fujimoto, T. Oku, T. Akiyama, Fabrication and characterization of ZnO/Cu_2O solar cells prepared by electrodeposition, Appl. Phys. Express 6 (2013) 086503, http://dx.doi.org/10.7567/APEX.6.086503.
[15] Z. Bai, J. Liu, F. Liu, Y. Zhang, Enhanced photoresponse performance of self-powered UV–visible photodetectors based on ZnO/Cu_2O/electrolyte heterojunctions via graphene incorporation, J. Alloys Compd. 726 (2017) 803–809, http://dx.doi.org/10.1016/j.jallcom.2017.08.035.
[16] N.H. Ke, L.T.T. Trinh, P.K. Phung, P.T.K. Loan, D.A. Tuan, N.H. Truong, C.V. Tran, L.V.T. Hung, Changing the thickness of two layers: i-ZnO nanorods, p-Cu_2O and its influence on the carriers transport mechanism of the p-Cu_2O/i-ZnO nanorods/n-IGZO heterojunction, Springerplus 5 (2016) 710, http://dx.doi.org/10.1186/s40064-016-2468-y.
[17] D. Guo, Y. Ju, Preparation of Cu_2O/ZnO p-n junction by thermal oxidation method for solar cell application, Mater. Today Proc. 3 (2016) 350–353, http://dx.doi.org/10.1016/j.matpr.2016.01.019.
[18] S.S. Jeong, A. Mittiga, E. Salza, A. Masci, S. Passerini, Electrodeposited ZnO/Cu_2O heterojunction solar cells, Electrochim. Acta 53 (2008) 2226–2231, http://dx.doi.org/10.1016/j.electacta.2007.09.030.
[19] S.S. Wilson, Y. Tolstova, D.O. Scanlon, G.W. Watson, H.A. Atwater, Interface Stoichiometry Control to Improve Device Voltage and Modify Band Alignment in ZnO/Cu_2O Heterojunction Solar Cells, 2014, pp. 3606–3610, http://dx.doi.org/10.1039/c4ee01956c.
[20] X. Wu, J. Liu, P. Huang, Z. Huang, F. Lai, G. Chen, L. Lin, P. Lv, W. Zheng, Y. Qu, Engineering crystal orientation of p-Cu_2O on heterojunction solar cells, Surf. Eng. 33 (2017) 542–547, http://dx.doi.org/10.1080/02670844.2017.1288342.
[21] N.M. Rosas-Laverde, A. Pruna, D. Busquets-Mataix, B. Marí, J. Cembrero, F. Salas Vicente, J. Orozco-Messana, Improving the properties of Cu_2O/ZnO heterojunction for photovoltaic application by graphene oxide, Ceram. Int. 44 (2018) 23045–23051, http://dx.doi.org/10.1016/j.ceramint.2018.09.107.
[22] Y. Lin, X. Li, D. Xie, T. Feng, Y. Chen, R. Song, H. Tian, T. Ren, M. Zhong, K. Wang, H. Zhu, Graphene/semiconductor heterojunction solar cells with modulated antireflection and graphene work function, Energy Environ. Sci. 6 (2013) 108–115, http://dx.doi.org/10.1039/C2EE23538B.
[23] A. Pruna, M.D. Reyes-Tolosa, D. Pullini, M.A. Hernandez-Fenollosa, D. Busquets-Mataix, Seed-free electrodeposition of ZnO bi-pods on electrophoretically-reduced graphene oxide for optoelectronic applications, Ceram. Int. 41 (2015) 2381–2388, http://dx.doi.org/10.1016/j.ceramint.2014.10.052.
[24] D. Li, J. Cui, H. Li, D. Huang, M. Wang, Y. Shen, ScienceDirect Graphene oxide modified hole transport layer for $CH_3NH_3PbI_3$ planar heterojunction solar cells, Sol. Energy 131 (2016) 176–182, http://dx.doi.org/10.1016/j.solener.2016.02.049.
[25] G. Riveros, D. Ramírez, A. Tello, R. Schrebler, R. Henríquez, H. Gómez, Electrodeposition of ZnO from DMSO solution: influence of anion nature and its concentration in the nucleation and growth mechanisms, J. Braz. Chem. Soc. 23 (2012) 505–512, http://dx.doi.org/10.1590/S0103-50532012000300018.
[26] C. Yilmaz, U. Unal, Hydrothermal–electrochemical growth of heterogeneous ZnO: Co films, Appl. Nanosci. 7 (2017) 343–354, http://dx.doi.org/10.1007/s13204-017-0579-6.
[27] H. Gómez, S. Cantillana, F.A. Cataño, H. Altamirano, A. Burgos, Template assisted electrodeposition of highly oriented ZnO nanowire arrays and their integration in dye sensitized solar cells, J. Chil. Chem. Soc. 59 (2014) 2447–2450, http://dx.doi.org/10.4067/S0717-97072014000200010.
[28] H. Gómez, S. Cantillana, G. Riveros, S. Favre, C.J. Pereyra, D. Ariosa, R.E. Marotti, E.A. Dalchiele, Growth of epitaxial zinc oxide thin films onto gallium nitride by electrodeposition from a dimethylsulfoxide based electrolytic solution, Int. J. Electrochem. Sci. 8 (2013) 10149–10162.
[29] J. Cembrero, M. Perales, M. Mollar, B. Marí, Obtención de columnas de ZnO. Variables a controlar (I), Boletín La Soc, Española Cerámica y Vidr 42 (2003) 379–397 http://boletines.secv.es/upload/20120217144806.20125155.pdf.
[30] P. Cembrero-Coca, J. Cembrero, D. Busquets-Mataix, M.A. Pérez-Puig, B. Marí, A. Pruna, Factorial electrochemical design for tailoring of morphological and optical properties of Cu_2O, Mater. Sci. Technol. (United Kingdom) 0836 (2017), http://dx.doi.org/10.1080/02670836.2017.1349595.
[31] F.F. Oliveira, M.P. Proenca, J.P. Araújo, J. Ventura, Electrodeposition of ZnO thin films on conducting flexible substrates, J. Mater. Sci. 51 (2016) 5589–5597, http://dx.doi.org/10.1007/s10853-016-9850-6.
[32] P.U. Londhe, N.B. Chaure, Effect of pH on the properties of electrochemically prepared ZnO thin films, Mater. Sci. Semicond. Process. 60 (2017) 5–15, http://dx.doi.org/10.1016/j.mssp.2016.12.005.
[33] Z. Mezine, A. Kadri, L. Hamadou, N. Benbrahim, A. Chaouchi, Electrodeposition of copper oxides (Cu_xO_y) from acetate bath, J. Electroanal. Chem. 817 (2018), http://dx.doi.org/10.1016/j.jelechem.2018.03.055.
[34] D.-C.C. Perng, J.-W.W. Chen, T.-T.T. Kao, R.-P.P. Chang, Cu_2O growth characteristics on an array of ZnO nanorods for the nano-structured solar cells, Surf. Coat. Technol. 231 (2013) 261–266, http://dx.doi.org/10.1016/j.surfcoat.2012.05.054.
[35] A. Venkatesan, E.S. Kannan, Highly ordered copper oxide (Cu_2O) nanopillar arrays using template assisted electrodeposition technique and their temperature dependent electrical characteristics, Curr. Appl. Phys. 17 (2017) 806–812, http://dx.doi.org/10.1016/j.cap.2017.03.005.
[36] B. Scharifker, G. Hills, Theoretical and experimental studies of multiple nucleation, Electrochim. Acta 28 (1983) 879–889, http://dx.doi.org/10.1016/0013-4686(83)85163-9.
[37] H. Lahmar, F. Setifi, A. Azizi, G. Schmerber, A. Dinia, On the electrochemical synthesis and characterization of p-Cu_2O/n-ZnO heterojunction, J. Alloys Compd. 718 (2017) 36–45, http://dx.doi.org/10.1016/j.jallcom.2017.05.054.
[38] W. Septina, S. Ikeda, M.A. Khan, T. Hirai, T. Harada, M. Matsumura, L.M. Peter, Potentiostatic electrodeposition of cuprous oxide thin films for photovoltaic applications, Electrochim. Acta 56 (2011) 4882–4888, http://dx.doi.org/10.1016/j.electacta.2011.02.075.

[39] B. Shi, B. Liu, J. Luo, Y. Li, C. Zheng, X. Yao, L. Fan, J. Liang, Y. Ding, C. Wei, D. Zhang, Y. Zhao, X. Zhang, Enhanced light absorption of thin perovskite solar cells using textured substrates, Sol. Energy Mater. Sol. Cells 168 (2017) 214–220, http://dx.doi.org/10.1016/j.solmat.2017.04.038.
[40] D. Pullini, A. Pruna, S. Zanin, D.B. Mataix, High-efficiency electrodeposition of large scale zno nanorod arrays for thin transparent electrodes, J. Electrochem. Soc. 159 (2012) E45, http://dx.doi.org/10.1149/2.093202jes.
[41] A. Pruna, Q. Shao, M. Kamruzzaman, J.A. Zapien, A. Ruotolo, Optimized properties of ZnO nanorod arrays grown on graphene oxide seed layer by combined chemical and electrochemical approach, Ceram. Int. 42 (2016) 17192–17201, http://dx.doi.org/10.1016/j.ceramint.2016.08.011.
[42] F.J. Manjón, SK.F L.R., Effect of pressure on phonon modes in wurtzite zinc oxide, High Press. Res. 22 (2002) 299–304, http://dx.doi.org/10.1080/08957950290012968.
[43] B. Marí, F.J. Manjón, M. Mollar, J. Cembrero, R. Gómez, Photoluminescence of thermal-annealed nanocolumnar ZnO thin films grown by electrodeposition, Appl. Surf. Sci. 252 (2006) 2826–2831, http://dx.doi.org/10.1016/j.apsusc.2005.04.024.
[44] S. Kundu, A facile route for the formation of shape-selective ZnO nanoarchitectures with superior photo-catalytic activity, Colloids Surf. A Physicochem. Eng. Asp. 446 (2014) 199–212, http://dx.doi.org/10.1016/j.colsurfa.2013.12.035.
[45] A. Pruna, Z. Wu, J.A. Zapien, Y.Y. Li, A. Ruotolo, Enhanced photocatalytic performance of ZnO nanostructures by electrochemical hybridization with graphene oxide, Appl. Surf. Sci. 441 (2018) 936–944, http://dx.doi.org/10.1016/j.apsusc.2018.02.117.
[46] X. Pan, M.Q. Yang, Y.J. Xu, Morphology control, defect engineering and photoactivity tuning of ZnO crystals by graphene oxide-a unique 2D macromolecular surfactant, Phys. Chem. Chem. Phys. 16 (2014) 5589–5599, http://dx.doi.org/10.1039/c3cp55038a.
[47] F.J. Manjón, B. Marí, J. Serrano, A.H. Romero, Silent Raman modes in zinc oxide and related nitrides, J. Appl. Phys. 97 (2005) 1–4, http://dx.doi.org/10.1063/1.1856222.